JOURNAL OF SOLID STATE CHEMISTRY 66, 242–250 (1987)

Ordered Magnetic Frustration

VI. Crystal and Magnetic Structures of the Inverse Weberites $ZnFeF_5(H_2O)_2$ and $MnFeF_5(H_2O)_2$ at 1.5 K from Powder Neutron Diffraction

Y. LALIGANT

Laboratoire des Fluorures (UA CNRS 449), Faculté des Sciences, Université du Maine, Route de Laval, 72017 Le Mans Cedex, France

J. PANNETIER

I.L.L. Avenue des Martyrs, 156X, 38042 Grenoble Cedex, France

AND G. FEREY*

Laboratoire des Fluorures (UA CNRS 449), Faculté des Sciences, Université du Maine, Route de Laval, 72017 Le Mans Cedex, France

Received June 4, 1986; accepted in final form June 14, 1986

The nuclear and the magnetic structures of the ferrimagnetic (T_c = 39.5(2) K) $MnFeF_5(H_2O)_2$ and of the antiferromagnetic (T_N = 9(2) K) $ZnFeF_5(H_2O)_2$ inverse weberites were solved by neutron powder diffraction at 50 and 1.5 K, respectively. The room temperature structures are confirmed and hydrogen atoms are located. Below the magnetic ordering temperature, the magnetic and nuclear cells are identical. For $MnFeF_5(H_2O)_2$ (space group *Imm*2), the Bertaut's modes are $+F_x$, $-G_z$, and $-F_x$, $+F_y$, $-G_z$ for Fe^{3+} and Mn^{2+} spins, respectively, with corresponding moments of 3.43(9) and 4.93(11) μ_B (R_{mag} = 0.087). For $ZnFeF_5(H_2O)_2$ (space group *Imm*2), the Bertaut's mode is G_y for Fe^{3+} spins, the moments being 3.78(5) μ_B (R_{mag} = 0.066). These results, which show the influence of the existence of a topologically frustrating triangular cationic subnetwork on the magnetic behavior of compounds, are compared to those previously obtained on $Fe^{2+}Fe^{3+}F_5(H_2O)_2$, which cumulate the different parameters that govern frustrated behavior: triangular network, different kinds of magnetic interactions, and anisotropy.

Introduction

The concept of frustration was introduced by Toulouse (*1*). For several years, we have developed experimental studies to illustrate this concept; they concern the magnetic structures of 3*d* transition metal fluorides and describe the different arrangements adopted by spins in antiferromagnetic interactions when the corresponding cations form a triangular subnetwork (*2–6*). $M^{2+}Fe^{3+}F_5(H_2O)_2$ compounds (M^{2+} = Mn, Fe, Zn) satisfy this condition. Their room temperature structure (*7–9*) is related to the weberite type $Na_2M^{2+}M'^{3+}F_7$ with, however, an inversion of the divalent and the tervalent ions between the two structures. The crystal chemistry of $MFeF_5(H_2O)_2$ compounds can be described by *trans* chains of corner-sharing FeF_6 octahedra linked together by $M^{2+}F_4(H_2O)_2$ octahedra (Fig. 1) (*19*), thus forming a triangular cat-

* To whom correspondence should be addressed.

0022-4596/87 $3.00

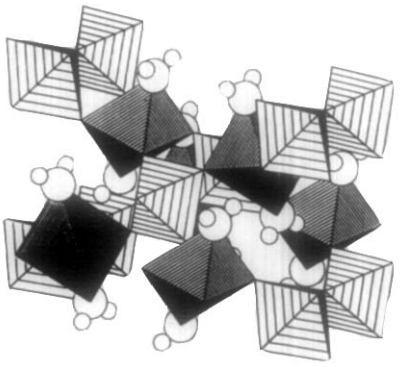

FIG. 1. Perspective view of the structure of the inverse weberite $MFeF_5(H_2O)_2$ · FeF_6 octahedra are lightly hatched.

ionic subnetwork in the (011) and (01$\bar{1}$) planes (Fig. 2).

Our previous study (*5*) of the ferrimagnet $Fe^{2+}Fe^{3+}F_5(H_2O)_2$ (T_c = 48.6(2) K) showed the existence of two magnetic structures above and below 26 K, in agreement with a previous Mössbauer (*10*) experiment which showed an anomaly in the thermal variation of the hyperfine field of Fe^{3+}. Above 26 K, the anisotropy of Fe^{2+} governs the exchange and obliges Fe^{3+} spins to adopt a parallel arrangement, although the Kanamori–Goodenough's rules (*17, 18*) predict only antiferromagnetic coupling; the latter progressively appears only below 26 K, and gives rise to a very complex magnetic structure, due both to frustrating triangular topology and to the anisotropy of Fe^{2+}.

These results induced us to first solve the magnetic structure of the ferrimagnet (T_c = 39.5(2) K) $MnFeF_5(H_2O)_2$ (*11, 12*) in order to show the frustrated arrangement of the spins when all the cations are in a d^5 configuration, i.e., when anisotropy is absent. By contrast, the corresponding study of the 1D antiferromagnet $ZnFeF_5(H_2O)_2$ (T_N = 9(2) K) (*12*) will describe the disposition of the spins when topological frustration is suppressed by introducing in an ordered manner a diamagnetic ion on one vertex of the triangle.

The format of this paper is as follows: we first give a brief description of the experimental procedures in section 1; in a second section, we present the structural characteristics of the compounds; in the third section, we describe the corresponding magnetic structures and, finally, compare the magnetic structures of the three inverse weberites in terms of frustration.

Experimental

Powder samples of $MFeF_5(H_2O)_2$ were prepared in large quantities by dissolution of either $MnCO_3$ or ZnO with freshly precipitated FeOOH in a boiling aqueous solution of 49% HF. Slow evaporation led to the desired products, which are filtered, washed with ethanol and ether, and air dried.

Neutron diffraction patterns were recorded above and below the magnetic ordering temperature for both compounds (50 and 1.5 K for $MnFeF_5(H_2O)_2$; 16 and 1.5 K for $ZnFeF_5(H_2O)_2$) on the D1B powder diffractometer of the HFR of the Institut Laue-Langevin (Grenoble), using a wavelength of 2.519 Å. Higher harmonic wavelengths were suppressed by a set of pyrolytic graphite filters. The samples were inserted in a cylindrical vanadium can (ϕ = 10 mm) held in a vanadium-tailed cryostat. For both samples the data were collected in

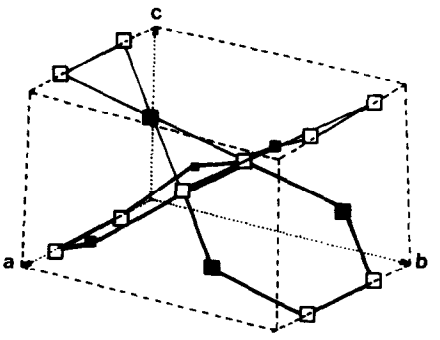

FIG. 2. Triangular cationic subnetwork of the inverse weberite.

the range $10° < \theta < 50°$ and correspond to 43 *hkl* triplets. Their analysis was performed with the Rietveld profile refinement method (*13*), as modified by Hewat (*14*). The nuclear scattering lengths and magnetic form factors were taken from (*15*) and (*16*), respectively.

Structural Study

(*1*) *$MnFeF_5(H_2O)_2$ at 50 K*

A previous single-crystal refinement at 300 K showed that $MnFeF_5(H_2O)_2$ is orthorhombic (a = 7.563(1) Å, b = 10.901(1) Å, c = 6.732(1) Å, Z = 4). The space group is *Imm*2, owing to the existence of some weak (*hk*0) reflections with *h* odd (*9*). The powder patterns recorded at 300 and 50 K are very similar and therefore rule out any structural phase transition between these two temperatures. Thus, the accurate atomic coordinates deduced from the single-crystal study were taken as starting values in the refinement; the primitive hydrogen positions were those determined during the previous neutron diffraction study of $Fe_2F_5(H_2O)_2$ (*5*). Owing to the high background due to the incoherent diffusion of hydrogen, isotropic thermal parameters were fixed at 0.20 Å^2 for cations, 0.65 Å^2 for F and O, and 1.24 Å^2 for H atoms. In these conditions, the refinement rapidly converges to R_{nuc} = 0.037; the resulting atomic coordinates and the corresponding distances and angles are listed in Tables I and II. They do not differ strongly from those at 300 K. Moreover, the location of hydrogen atoms permits one to specify the geometry of H_2O molecules which is in good agreement with their common values.

TABLE I

CELL PARAMETERS AND ATOMIC COORDINATES OF $MnFeF_5(H_2O)_2$ AT 50 K

SG *Imm*2	a = 7.475(1) Å	b = 10.766(1) Å	
	c = 6.594(1) Å	z = 4	
Atom	x	y	z	B
Mn(4)	0	$\frac{3}{4}$	$\frac{3}{4}$	0.20
Fe(4)	$\frac{1}{4}$	0	0	0.20
F1	0.291(1)	0.873(1)	0.198(1)	0.65
F2	0.709(1)	0.626(1)	0.302(1)	0.65
F3	0	0	0.073(1)	0.65
F4	0	$\frac{1}{2}$	0.427(4)	0.65
O1	$\frac{1}{2}$	0.321(2)	0.945(3)	0.65
O2	$\frac{1}{2}$	0.179(2)	0.554(4)	0.65
H1	0.101(2)	0.840(4)	0.363(3)	1.24
H2	0.897(2)	0.660(2)	0.138(3)	1.24

Note. R_{F^2} = 3.74%, R_{prof} = 10.18%, R_{wp} = 6.72%, R_{exp} = 5.21%, R_{nuc} = 3.74%.

(*2*) *$ZnFeF_5(H_2O)_2$*

Here also, no structural change is detected at low temperature. The 16 K pattern exhibits, below the Bragg peaks, broad diffusion peaks which confirm the 1D magnetic dimensionality and rule out any accurate refinement of the data. Thus, they were refined simultaneously with the magnetic data from the 1.5 K pattern. However, in this pattern, a new peak (110) appears, which excludes the space group *Imma*, even though this reflection is mainly magnetic in origin. The refined values of the preceding structure were taken as starting coordinates for the refinement which easily converges to R_{nuc} = 0.030, the thermal parameters being fixed, for the same reason as above, at values indicated in Table III. Tables III and IV summarize the final values of coordinates, distances, and angles. Despite a good *R*-factor, it is noteworthy that, for this structure, the distances are rather inhomogeneous, but the mean approximately corresponds to the sum of ionic radii (*20*).

Magnetic Structures

(*1*) *$MnFeF_5(H_2O)_2$*

Below T_c, new magnetic peaks appear which can be indexed in the nuclear cell

TABLE II

INTERATOMIC DISTANCES (Å) AND BOND ANGLES (°) OF $MnFe_5(H_2O)_2$ AT 50 K

Mn^{2+} octahedron					
Mn–F1	2 × 2.077	F1–F1	3.120	F1–Mn–F1	97.41
Mn–F2	2 × 2.079	F1–F2	2 × 2.742	F1–Mn–F2	82.56
Mn–O1	2.152	F1–O1	2 × 3.098	F1–Mn–O1	94.19
Mn–O2	2.146	F1–O2	2 × 2.874	F1–Mn–O2	85.80
		F2–F2	3.125	F2–Mn–F2	97.47
		F2–O1	2 × 2.981	F2–Mn–O1	85.83
		F2–O2	2× 3.095	F2–Mn–O2	94.18
Fe^{3+} octahedron					
Fe–F1	2 × 1.914	F1–F1	2.729	F1–Fe–F1	90.95
Fe–F2	2 × 1.912	F1–F2	2.682	F1–Fe–F2	89.03
Fe–F3	1.930	F1–F3	2.698	F1–Fe–F3	89.19
Fe–F4	1.930	F1–F4	2.738	F1–Fe–F4	90.83
		F2–F2	2.728	F2–Fe–F2	90.92
		F2–F3	2.737	F2–Fe–F3	90.88
		F2–F4	2.696	F2–Fe–F4	89.10
		F3–F4	3.860		
Superexchange angles and metal–metal distances					
Fe–F3–Fe	151.12	Mn–F1–Fe	133.57		
Fe–F4–Fe	151.05	Mn–F2–e	133.72		
Fe–Fe	3.737	Mn–Fe	3.667		
Water molecules					
O1–H1	0.952	H1–O1–H1	105.54		
H1–H1	1.516				
O2–H2	0.965	H2–O2–H2	104.50		
H2–H2	1.525				

Note. e.s.d.'s are smaller than 0.010 Å for distances and 0.4° for angles.

with the same I lattice. Therefore, the identity of the nuclear and magnetic cells permits Bertaut's macroscopic theory to be used (*21*). 2_z, m_{1a}, and I translation are taken as the three independent symmetry elements. If R_i and S_i ($i = 1, 4$) represent the magnetic moments of Fe^{3+} and Mn^{2+} corresponding to the atomic coordinates reported in Table V, it is possible to define in each sublattice four linear combinations of the moments $F = M_1 + M_2 + M_3 + M_4$, $G = M_1 - M_2 + M_3 - M_4$, $C = M_1 + M_2 - M_3 - M_4$, $A = M_1 - M_2 - M_3 + M_4$ ($M = R, S$) which represent the ferromagnetic and the antiferromagnetic modes of coupling. The basis vectors, in the irreducible representation of space group *Imm*2, lead to eight modes, but only two of them (Γ_1 and Γ_2) are compatible with the magnetization of both Fe^{3+} and Mn^{2+} sublattices and also with ferrimagnetism (Table V).

Retaining the refined coordinates of the 50 K pattern the best fit ($R_{mag} = 0.087$) between observed and calculated intensities correspond to the Γ_2 mode: $+F_x$, $-G_z$ and $-F_x$, $+F_y$, $-G_z$ for Fe^{3+} and Mn^{2+} components, respectively. All the other combinations of signs lead to an increase of the mag-

netic R-factor. The components of the magnetic moments R and S on the axes of the cell are listed in Table VI. The comparison of the observed and calculated profiles appear in Fig. 3. Our results lead to a star magnetic structure in which the angles between the spins, also shown in Table VI, differ significantly from 120°. Ferrimagnetism results both from the opposite signs of the F_x components of Fe^{3+} and Mn^{2+}, and from the absence of the F_y component for the Fe^{3+} sublattice, whereas it exists for that of Mn^{2+}. The resulting calculated moment (μ = 2.89 μ_B) is in good agreement with the saturated moment deduced from magnetization measurements (μ = 2.5(1) μ_B). The corresponding magnetic dipolar energy appears in Table VII. The lattice summation was carried out in the real space within a sphere of 100 Å radius; it shows that the Fe^{3+}–Mn^{2+} contribution predominates. This is in agreement with the relatively low value of the moment of Fe^{3+}, as compared to that of Mn^{2+}.

TABLE III

CELL PARAMETERS AND ATOMIC COORDINATES OF $ZnFeF_5(H_2O)_2$ AT 3.5 K (*Imm2*)

a = 7.451(1) Å b = 10.747 Å
c = 6.524 Å z = 4

	x	y	z	B (Å)^2
Zn	0	$\frac{1}{4}$	$\frac{3}{4}$	0.25
Fe	$\frac{1}{4}$	0	0	0.25
F1	0.274(1)	0.872(1)	0.222(4)	0.57
F2	0.687(1)	0.624(1)	0.316(3)	0.57
F3	0	0	0.065(6)	0.57
F4	0	$\frac{1}{2}$	0.401(4)	0.57
O1	$\frac{1}{2}$	0.307(4)	0.968(6)	0.57
O2	$\frac{1}{2}$	0.183(4)	0.566(6)	0.57
H1	0.120(5)	0.843(4)	0.389(6)	0.67
H2	0.908(4)	0.669(5)	0.131(5)	0.67

Note. R_{F^2} = 3.41%, R_p = 6.38%, R_{wp} = 4.71%, R_{exp} = 3.40%, R_{nuc} = 2.96%, R_{mag} = 6.63%.

(2) $ZnFeF_5(H_2O)_2$

As already mentioned, the existence of the (110) purely magnetic reflection at 1.5 K excludes the *Imma* group as a magnetic one; this suggests at least the magnetic space groups of *Imm*2, if the orthorhombic magnetic symmetry is preserved, or its monoclinic subgroups.

As indicated in Table V, the sublattice of Fe^{3+} leads to antiferromagnetism only with five modes Γ_1, Γ_5, Γ_6, Γ_7, Γ_8. Only Γ_1, which predicts a strict antiferromagnetic arrangement of the spins of Fe^{3+} along y, yields satisfactory results (μ = 3.78(5) μ_B, R_{mag} = 0.066), the four others yielding unacceptably high magnetic R (>0.40) values. Refinements in the magnetic subgroups do not improve the results, which lead to pure antiferromagnetism between Fe^{3+} ions in the chains, the spins being orthogonal to the direction of these chains. The corresponding magnetic dipolar energy is −0.506 J mole^{-1}.

Discussion

The first conclusion of this study relates once more to the importance of the geometry of the antiferromagnetic cationic sublattice on the magnetic behavior: when it involves isolated strings, as in $ZnFeF_5(H_2O)_2$, 1D antiferromagnetic behavior is observed, with spins strictly antiparallel; when the strings are linked by supplementary magnetic cations to form a triangular metallic network (as is the case for $MnFeF_5(H_2O)_2$), the "natural" antiferromagnetism cannot be maintained. When all the spins are identical, this leads to star structures in which the angles are equal (*6*) or different from 120° The former case gives rise to antiferromagnetism (HTB FeF_3); the latter case occurs for $MnFeF_5(H_2O)_2$ and leads to the observed ferrimagnetism, really unusual for a compound in which all the cations are in d^5

TABLE IV

INTERATOMIC DISTANCES (Å) AND BOND ANGLES (°) OF $ZnFeF_5(H_2O)_2$ AT 1.5 K

Zn^{2+} octahedron					
Zn–F1	2 × 2.139	F1–F1	3.364	F1–Zn–F1	103.67
Zn–F2	2 × 1.987	F1–F2	2 × 2.748	F1–Zn–F2	83.41
Zn–O1	1.934	F1–O1	2 × 3.043	F1–Zn–O1	96.53
Zn–O2	2.187	F1–O2	2 × 2.866	F1–Zn–O2	82.95
		F2–F2	2.781	F2–Zn–F2	88.78
		F2–O1	2 × 2.757	F2–Zn–O1	89.36
		F2–O2	2 × 2.987	F2–Zn–O2	91.24
Fe^{3+} octahedron					
Fe–F1	2 × 2.007	F1–F1	2.754	F1–Fe–F1	86.62
Fe–F2	2 × 1.855	F1–F2	2.730	F1–Fe–F2	89.36
Fe–F3	1.911	F1–F3	2.667	F1–Fe–F3	85.75
Fe–F4	1.969	F1–F4	3.016	F1–Fe–F4	98.63
		F2–F2	2.666	F2–Fe–F2	91.83
		F2–F3	2.523	F2–Fe–F3	84.03
		F2–F4	2.746	F2–Fe–F4	91.72
		F3–F4	3.875		
Superexchange angles and metal–metal distances					
Fe–F3–Fe	154.13	Zn–F1–Fe	123.48		
Fe–F4–Fe	142.02	Zn–F2–Fe	143.82		
Fe–Fe	3.725	Zn–Fe	3.653		
Water molecules					
O1–H1	1.107	H1–O1–H1	108.44		
H1–H1	1.797				
O2–H2	0.820	H2–O2–H2	113.3		
H2–H2	1.370				

Note. e.s.d.'s are smaller than 0.010 Å for distances and 0.4° for angles.

states. The spins are strongly canted (115.7° between two Fe^{3+} instead of 180° for the Zn compound) and some of the magnetic moments are weakened.

In addition to this evidence for the role of the triangular sublattice in frustrated magnetic behavior, it is interesting to undertake a comparison (Fig. 4) with the ferrous compound $Fe^{2+}Fe^{3+}F_5(H_2O)_2$ (*10*). Instead of the isotropic Mn^{2+} ion, Fe^{2+} introduces its own strong anisotropy and also produces a disparity in the strengths of interactions in the triangle. This results in two magnetic structures above and below 26 K. At higher temperatures, the magnetic structure is completely governed by the anisotropy of Fe^{2+} whose magnetic moment saturates very rapidly below $T_c = 48.6$ K. The Fe^{2+}–Fe^{3+} interactions are the most important, and oblige the spins of Fe^{3+} to adopt a parallel arrangement, and then a complete frustration of their antiferromagnetic coupling, predicted by the Kanamori–Goodenough's rules. It is only below 26 K that, progressively, the Fe^{3+}–Fe^{3+} *AF* interaction appears and becomes predominant at

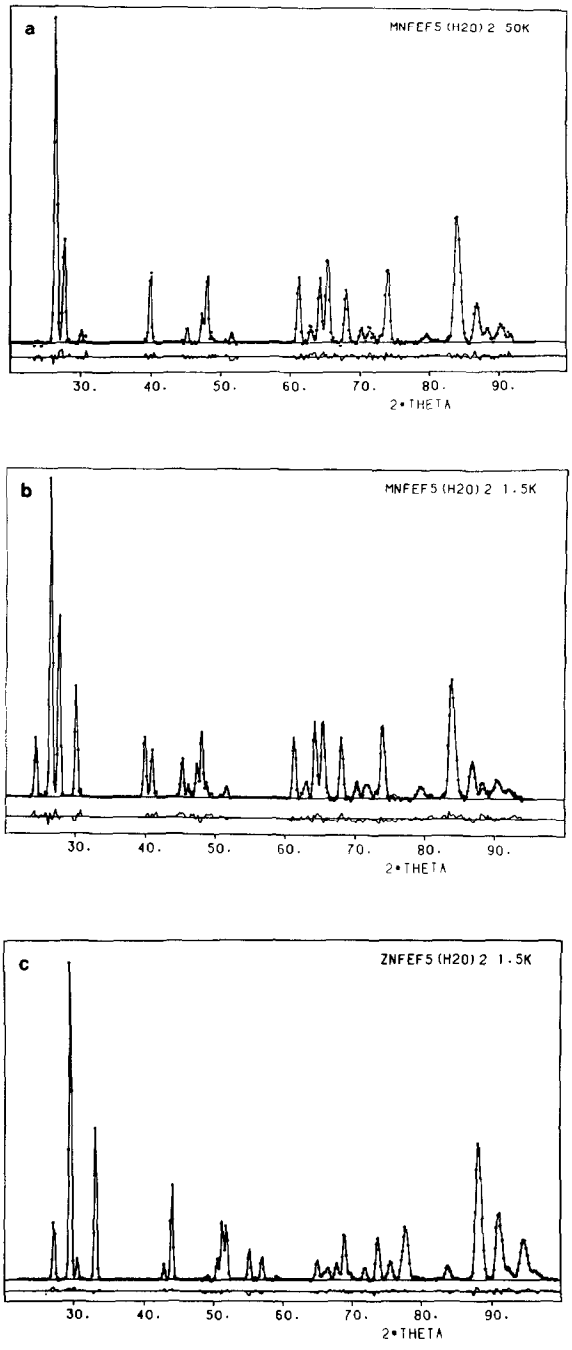

FIG. 3. Comparison of the observed and calculated profiles of $MnFeF_5(H_2O)_2$ at 50 K (a), 5 K (b), and of $ZnFeF_5(H_2O)_2$ at 1.5 K.

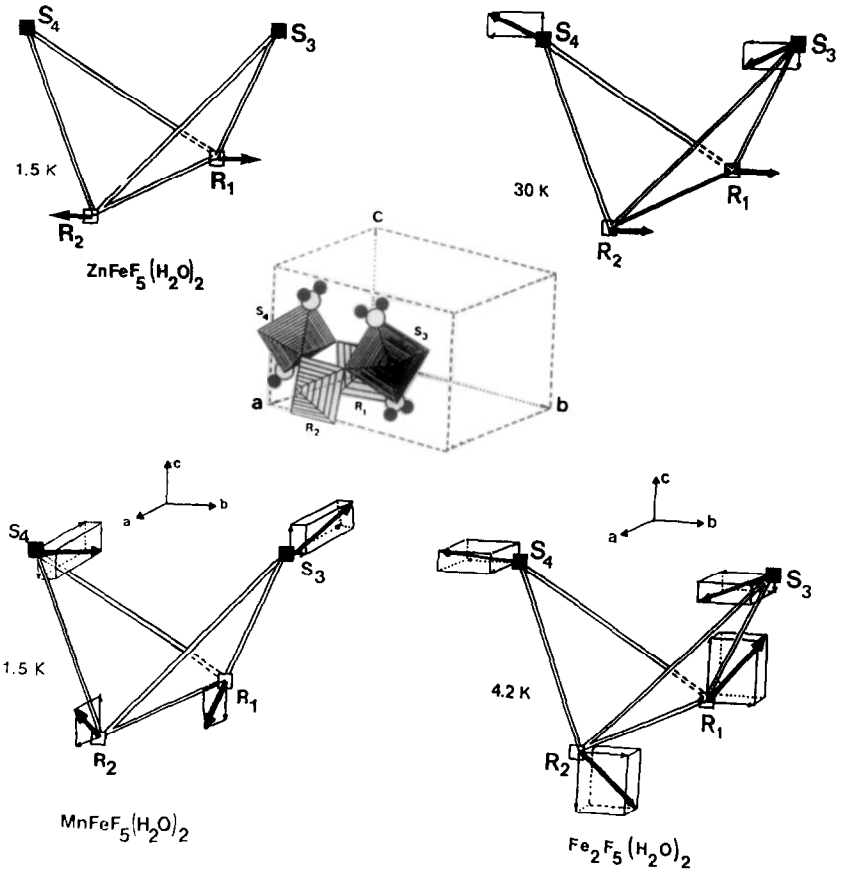

FIG. 4. Comparison of the disposition of the spins in the double cationic triangle $R_1R_2S_3S_4$ for $ZnFeF_5(H_2O)_2$ (a), $MnFeF_5(H_2O)_2$ (b), and $Fe_2F_5(H_2O)_2$ at 30 K (c) and 4.2 K (d).

TABLE V

ATOMIC COORDINATES OF THE SPINS OF Fe^{3+} (R_i) AND M^{2+} (S_i) AND CORRESPONDING MAGNETIC MODES IN SPACE GROUP *Imm*2

Fe^{3+}				M^{2+}			
$\vec{R_1}$	$\frac{1}{4}$	0	0	$\vec{S_1}$	0	0.25	0.75
$\vec{R_2}$	$\frac{3}{4}$	0	0	$\vec{S_2}$	0	0.75	0.75
$\vec{R_3}$	$\frac{3}{4}$	$\frac{1}{2}$	$\frac{1}{2}$	$\vec{S_3}$	$\frac{1}{2}$	0.75	0.25
$\vec{R_4}$	$\frac{1}{4}$	$\frac{1}{2}$	$\frac{1}{2}$	$\vec{S_4}$	$\frac{1}{2}$	0.25	0.25

Mode						
2z.m.I	x	y	z	x	y	z
Γ_1 (+++)	.	Gy	.	Gx	Gy	Fz
Γ_2 (−++)	Fx	.	Gz	Fx	Fy	Gz
Γ_3 (−−+)	.	Fy	.	.	.	.
Γ_4 (+−+)	Gx	.	Fz	.	.	.
Γ_5 (−+−)	Cx	.	Az	Cx	Cy	Az
Γ_6 (−−−)	.	Cy	.	.	.	.
Γ_7 (+−−)	Ax	.	Cz	.	.	.
Γ_8 (++−)	.	Ay	.	Ax	Ay	Cz

TABLE VI

REFINED VALUES OF THE COMPONENTS OF THE MAGNETIC MOMENTS IN THE *Imm*2 GROUP (T = 1.5 K MOMENTS IN μB) AND ANGLES OF SPIN CANTING

Rx	Ry	Rz	$\lvert\vec{R}\rvert$	Sx	Sy	Sz	$\lvert\vec{S}\rvert$	R_{nuc}	R_{mag}	R_p	R_{wp}	R_{exp}
1.83	0	−2.90	3.43	−4.59	0.86	−1.60	4.93	6.09	8.70	11.1	7.83	5.55

Fe–Fe in the chain	115.7 ($R_1 \cdot R_2$)
Mn–Fe	140.2 ($S_3 \cdot R_1$)
	102.8 ($S_3 \cdot R_2$)

TABLE VII

MAGNETIC DIPOLAR ENERGY (J · m^{-1})

Contribution of → / on ↓	Mn^{2+}	Fe^{3+}	Mn^{2+} + Fe^{3+}
Mn^{2+}	−0.158	−0.840	−0.998
Fe^{3+}	−0.840	−0.638	−1.478

4.2 K, giving rise to a magnetic structure similar to that of $MnFeF_5(H_2O)_2$. The comparison of the magnetic structures of the three inverse weberites thus sheds some light on the different situations which can occur when frustration is present.

References

1. TOULOUSE, G., *Comm. Phys.* **2,** 115 (1977).
2. FEREY, G., DE PAPE, R., AND BOUCHER, B., *Acta Crystallogr. Sect. B* **34,** 1084 (1978).
3. FEREY, G., LEBLANC, M., DE PAPE, R., AND PANNETIER, J., *Solid State Commun.* **53**(6), 559 (1985).
4. FEREY, G., LEBLANC, M., DE PAPE, R., AND PANNETIER, J., Competing interactions and spin frustration problems in fluorides," *in* "Inorganic fluorides: Chemistry and physics." (P. Hagenmuller, Ed.), p. 395, Academic Press (1985).
5. LALIGANT, Y., LEBLANC, M., PANNETIER, J., AND FEREY, G., *J. Phys. C* **19,** 1081 (1986).
6. LEBLANC, M., PANNETIER, J., DE PAPE, R., FEREY, G., *Solid State Commun.*, **58,** 171 (1986).
7. HALL, W., KIM, S., ZUBIETA, J., WALTON, E. G., AND BROWN, D. B., *Inorg. Chem.* **16,** 1884 (1977).
8. LALIGANT, Y., PANNETIER, J., LABBE, P., AND FEREY, G., *J. Solid State Chem.*, **62,** 274 (1986).
9. LALIGANT, Y., PANNETIER, J., LEBLANC, M., LABBE, P., AND FEREY, G., *Z. Kristallogr.*, in press.
10. IMBERT, P., JEHANNO, G., MACHETEAU, AND VARRET, F., *J. Phys. (Paris)* **37,** 969 (1976).
11. JONES, E. R., VAN HINE, C., DATTA, T., CATHEY, L., AND KARRAKER, D. G., *Inorg. Chem.* **24,** 3888 (1985).
12. LALIGANT Y., CALAGE, Y., TORRES-TAPIA, E., VARRET, F., AND FEREY, G., *J. Magn. Magn. Mater.*, submitted.
13. RIETVELD, H. M., *J. Appl. Crystallogr.* **2,** 65 (1969).
14. HEWAT, A. W., Harwell Report AERE, R 7350 (1973), *Acta Crystallogr. Sect. A* **35,** 248 (1979).
15. KOESTER, L., AND RAUCH, H., IAEA Contract 2517/RB (1981).
16. WATSON, R. E., AND FREEMAN, J., *Acta Crystallogr.* **14,** 27 (1961).
17. KANAMORI, J., *J. Phys. Chem. Solids* **10,** 87 (1959).
18. GOODENOUGH, J. B., "Magnetism and the Chemical Bond," Interscience, New York (1963).
19. FISCHER, R. X., Program STRUPLO, *J. Appl. Crystallogr.* **18,** 258 (1985).
20. SHANNON, R. D., *Acta Crystallogr. Sect. A* **32,** 751 (1976).
21. BERTAUT, E. F., *in* "Magnetism III" (Rado-Shull, Eds.) (1963).